DEXTEROUS TASK-PRIORITY BASED REDUNDANCY RESOLUTION FOR UNDERWATER-MANIPULATOR SYSTEMS

Serdar Soylu, Bradley J. Buckham*, and Ron P. Podhorodeski
Department of Mechanical Engineering,
University of Victoria, P.O. Box 3055, Victoria, B.C., Canada, V8W 3P6
{serdar, bbuckham, podhoro}@me.uvic.ca
*Corresponding author: Fax: (250) 721-6035

ABSTRACT

The problem of redundancy resolution for underwater remote vehicle-manipulator systems (**URVM**) is addressed in the current work. In URVM applications, it is beneficial to have the underwater remote vehicle (**URV**) hold station using its thrusters while a human pilot operates the serial manipulator. This provides a stable platform for the manipulator and eases the pilot's job drastically when current and/or tether disturbances are present. However, when following this objective, the redundancy of the URVM as a whole is wasted; the four actively controlled motions of the URV are not used to improve the efficacy of the manipulator task. In fact, this standard operating procedure frequently puts the manipulator into near singular configurations. This is not desirable from the manipulator controller standpoint since near singular configurations result in undesirably high joint velocities and oscillations. In this work, a new heuristic approach based on the task-priority redundancy resolution scheme is applied to the URVM. The proposed approach provides a means to avoid singular configurations of the manipulator, and provides dexterous manipulation by using the URV's mobility in an optimal, coordinated manner. This scheme is particularly useful for remote systems where an a priori trajectory generator is not applicable. Numerical case studies are developed to demonstrate the effectiveness of the proposed technique.

RÉSUMÉ

RÉSOLUTION REDONDANTE BASÉE SUR LA PRIORITÉ POUR LES SYSTÈMES DE MANIPULATEURS SOUS-MARINS POUR TÂCHES HABILES

Le problème de la résolution redondante pour les systèmes de manipulateurs-véhicule sous-marin télé-commandés (MVST) est résolu dans le travail présent. Dans les aplications des MVST, il est bénéfique que le véhicule sous-marin télé-commandé (VST) maintienne sa position avec ses propulseurs tandis qu'un pilote humain actionne le manipulateur sériel. Cela fourni une plate-forme stable pour le manipulateur et facilite radicalement la tâche du pilote en présence de dérangements dus au courrant et/ou au cordon ombilical. Cependant, en poursuivant cet objectif, la redondance du MVST est gâchée: les quatres déplacements activement controllés par le VST ne sont pas utilisés pour augmenter l'efficacité de la tâche manipulateur. En fait, cette procédure habituelle d'opération place fréquement le manipulateur en configurations quasi-singulières. Cela n'est pas souhaitable du point de vue du controleur du manipulateur car lorsque le système est proche d'une configuration singulière, des vitesses de jointure élevées et des oscillations involontaires se produisent. Dans ce travail, une nouvelle approche heuristique basée sur le schéma de résolution redondante des priorités de tâche est appliquée au MVST affin de concilier différents objectifs avec les degrés de liberté collectifs du MVST. La méthode permet d'augmenter la dextérité de la composante manipulateur du MVST, en utilisant les déplacements du VST pour améliorer le positionnement du manipulateur, tout en maitenant les déplacements du VST à un minimum. Des études de cas numériques sont développées pour présenter l'efficacité de la technique proposée.

1 INTRODUCTION

Underwater remote vehicles (**URVs)** equipped with robotic manipulators play an important role in a number of shallow and deep-water missions for marine science, oil and gas extraction, exploration and salvage [1]. In these applications, the URV is used as a mobile platform that delivers the robotic manipulator to a subsea work site. The motions of the URV and the manipulator are guided independently by a human pilot on a surface support vessel through a long slender tether that provides power and telemetry. For detailed surveys, the URV motion can be accomplished by an on-board URV controller. These controllers use URV state feedback provided by acoustic and inertial positioning systems [2], and dynamic models to intelligently control the conventional thrusters arranged on the URV chassis. Manipulator units are generally add-on technologies produced by independent manufacturers, and hence the manipulator most often has an independent control system. The desired manipulator joint motions are created using a teleoperated master-slave arm configuration. Driving the passive master-arm, the human pilot sets the desired end-effector position and orientation that is to be duplicated by the submerged slave arm, provided the URV can hold station.

However, during the URV manoeuvre, the pilot encounters enormous difficulties. The URV thrusters rely on momentum transfer to a fluid and have an inherent lag in their response to pilot inputs. Furthermore, URV's are bluff bodies designed for omnidirectional operation and have poor drag characteristics, which slow the response of the URV to the pilot's command. As such, the manipulator joints are relied upon for detailed interaction with the subsea environment, while the URV thrusters are generally used to try and counter tether and current disturbances. However, this URV functionality is compromised by the limited visual and navigational feedback available to the pilot, and the subsequent inability to sense disturbances being exerted by the tether and the current. Furthermore, when the movement is replicated by the slave arm, the inertial and hydrodynamic drag associated with the manipulator links create reactions at the manipulator-URV junction. The reaction loads act as disturbances to the URV motion which in turn disturbs the placement of the end-effector [1, 4]. These factors make it very difficult for an individual to synchronize the thrusters and manipulator commands, and often two pilots will work together during deployment.

It is proposed that the URV and the manipulator motion be coordinated such that a consolidated controller amalgamates URV navigation data, manipulator state feedback, and a single pilot command to achieve a desired end-effector motion. The consolidated system is referred to as an underwater remote vehicle-manipulator (**URVM**). By coordinating the collective degrees of freedom of the URVM in response to a single pilot input the operator would only be concerned with driving the end-effector, the URVM efficacy would be greatly improved, and the scope of the detailed operations required by projects such as VENUS and NEPTUNE, which involves setting up a cable-linked seafloor observatory, would become possible.

In addition to the manipulator revolute joints, the URV itself contributes four active degrees of freedom, including surge (forward), sway (lateral) and heave (vertical) translations, and a yawing rotation about the vertical axis. Also, the URV is a free-floating body, and thus moves in two additional rotations: pitch and roll. However, these motions are not controlled, but rather are mitigated by a strong buoyant restoring moment. Due to its kinematic redundancy, the URVM system admits an infinite number of joint-space solutions for a given end-effector position and orientation. This allows one to use the available redundancy to achieve additional objectives besides the given end-effector task using a redundancy resolution technique. The primary objective is to coordinate the URV and the manipulator motion for a given end-effector path, and eliminate the need for the pilot intervention in the URV motion. In addition to that, various optimization criteria (e.g., reduction of fuel consumption, increase of system manipulability), can be fulfilled by using those degrees of freedom not needed in the satisfaction of the primary objective.

In URVM applications, there are additional constraints not present in most land-based redundant manipulators. These constraints are mostly due to the dynamics of the URV: it is not always desirable to use the URV surge, sway, heave, and yaw motions extensively in placing the end-effector for several

reasons. Firstly, the small URV movements cause significant changes in the end-effector location since the small URV motions are amplified by the link lengths. Secondly, the URV consumes relatively more energy than the manipulator for a given motion due to its larger inertia [3, 5, 6]. The consideration of the large inertia of the URV is important since the redundancy resolution scheme could ask the URV to move in a manner that is not possible. Thirdly, the control of the URV is relatively more difficult since its response time is much slower [3].

The implementations of redundancy resolution methods to the URVM systems have been documented in only a few existing works [5]. The singularity robust task-priority redundancy resolution [7], which was originally proposed in [8] and [9], was shown to be effective for a URVM in [6] due to its multitask capabilities. In [10], the kinematic redundancy is utilized to minimize the total hydrodynamic drag forces experienced by a URVM system in an effort to reduce the energy consumption. However, the different dynamic characteristics of the URV and the manipulator were not addressed. In [5], the singularity robust task-priority redundancy resolution is merged with a fuzzy technique to resolve the URV-manipulator coordination. It was shown that the fuzzy method provides a versatile tool to handle multiple secondary tasks. In the same paper, it was also shown that the task priority fuzzy approach can be used to keep the vehicle stationary in an attempt to provide a stable platform for the manipulator and to reduce the energy consumption. Among the existing redundancy resolution schemes for the URVM systems, the task-priority approach is prominent. However, the direct implementation of the task-priority approach presented in prior works consistently forces the manipulator to work in, or near, degenerate configurations resulting in undesirably high joint velocities and oscillations. The solution to this problem requires either complex fuzzy rules or a priori trajectory knowledge [5, 6]. Also, unlike a redundant land-based manipulator, the redundancy of the URVM can not be relied upon when the manipulator hits degeneracy: the response time of the URV motions may not meet that of the subsequent pilot end-effector command. In addition, if the URVM finishes a task in a singular configuration such as when the manipulator is stretched out, and the next task is to lift a heavy object, then it may be impossible to lift up the material without exceeding the actuator torque limit, or the righting moment provided by the URV buoyancy module. To circumvent these potential problems, the URV mobility can be freed to provide only the slow motion of the manipulator base in an attempt to increase the dexterity of the manipulator, and move away from singular configurations.

In the current work, it is shown that the direct implementation of the singularity robust task-priority approach of [7] is not suitable for URVM applications since it causes the manipulator component to fall into its singular configurations. To overcome this problem, a new heuristic approach to the redundancy resolution problem of URVM systems is presented. The proposed approach is a variation of the task-priority redundancy resolution. In this method, low priority secondary tasks attempt to exploit slow URV motions and an increase in the system manipulability is sought when necessary. An on-line solution for the occurrence of algorithmic and kinematic singularities is used. To this end, measure of manipulability is used to gauge proximity to singular configurations. This scheme is particularly useful for remote systems where an a priori trajectory generator is not applicable.

2 THEORETICAL BACKGROUND

2.1 Forward Velocity Problem

The task-space velocity vector $\dot{\mathbf{x}} \in \mathbb{R}^m$ and joint-space velocity vector $\dot{\mathbf{q}} \in \mathbb{R}^n$ are related by:

$$\dot{\mathbf{x}} = \mathbf{J}\dot{\mathbf{q}} \tag{1}$$

where $\mathbf{J} = \partial \mathbf{f} / \partial \mathbf{q} \in \mathbb{R}^{m \times n}$ is the Jacobian matrix. For a kinematically redundant manipulator, $(n > m)$ and there are an infinity set of joint rates solution that can complete the desired end-effector motion, $\dot{\mathbf{x}}$. The existing solution procedures for Eq. (1) apply additional constraints in order to create a deterministic set of equations. The methods are distinguished by the influence of these constraint equations.

2.2 Pseudo Inverse Solution

The minimum-norm solution to the inverse kinematics problem associated with Eq. (1) minimizes $\|\dot{\mathbf{x}} - \mathbf{J}\dot{\mathbf{q}}\|_2$ and $\|\dot{\mathbf{q}}\|_2 = \sqrt{\dot{\mathbf{q}}^T\dot{\mathbf{q}}}$, and is given by:

$$\dot{\mathbf{q}} = \mathbf{J}^{\dagger}\dot{\mathbf{x}} \tag{2}$$

where $\mathbf{J}^{\dagger} = \mathbf{J}^T\left(\mathbf{J}\mathbf{J}^T\right)^{-1}$ is called the right Moore-Penrose pseudoinverse [11]. However, this solution does not guarantee singularity avoidance.

2.3 Projected Gradient Method

A general solution to Eq. (1), that sacrifices the minimum norm properties, can be obtained by adding a null space solution to the minimum-norm solution [11]:

$$\dot{\mathbf{q}} = \mathbf{J}^{\dagger}\dot{\mathbf{x}} + \left(\mathbf{I} - \mathbf{J}^{\dagger}\mathbf{J}\right)\dot{\mathbf{q}}_0 \tag{3}$$

where $\dot{\mathbf{q}}_0 \in \mathbb{R}^n$ is an arbitrary joint velocity vector. The term $\left(\mathbf{I} - \mathbf{J}^{\dagger}\mathbf{J}\right)$ is called the projection operator, and it projects the vector $\dot{\mathbf{q}}_0$ onto the null space of the end effector Jacobian matrix. The resulting null-space velocities generate motions within the serial manipulator that do not produce any end-effector motion. Thus, these "internal" motions can be exploited to achieve additional objectives. Liegeois [12] proposed that the arbitrary vector $\dot{\mathbf{q}}_0$ be the gradient of a scalar objective (potential) function $h(\mathbf{q})$:

$$\dot{\mathbf{q}} = \mathbf{J}^{\dagger}\dot{\mathbf{x}} + \left(\mathbf{I} - \mathbf{J}^{\dagger}\mathbf{J}\right)\left(\lambda\nabla h(\mathbf{q})\right) \tag{4}$$

where negative values of the scalar gain λ minimize $h(\mathbf{q})$, and positive values maximize this objective function. Equation (4) is called the projected gradient method.

2.4 Task Priority Redundancy Resolution

The task priority redundancy resolution technique attempts to divide a required task into subtasks according to the order of priority [8, 9]. To resolve conflicting directives from the multiple tasks, a hierarchy is established such that subtasks with lower priority are realized using extra degrees of freedom that are not taken by higher priority subtasks. When conflicts between tasks arise, the solution that is in favour of the higher priority task is realized.

The task priority redundancy resolution technique can be viewed as a variation of the projection gradient method. Instead of projecting the gradient of a scalar objective function through the projection operator, lower priority tasks are sequentially projected onto the null space of higher priority tasks. For the sake of simplicity, consider a double-task case in which the primary task $\dot{\mathbf{x}}_p \in \mathbb{R}^{m_1}$ has high priority, and the secondary task $\dot{\mathbf{x}}_s \in \mathbb{R}^{m_2}$ has low priority.

$$\dot{\mathbf{x}}_p = \mathbf{J}_p\dot{\mathbf{q}} \tag{5}$$

$$\dot{\mathbf{x}}_s = \mathbf{J}_s\dot{\mathbf{q}} \tag{6}$$

where $\mathbf{J}_p \in \mathbb{R}^{m_1 \times n}$ and $\mathbf{J}_s \in \mathbb{R}^{m_2 \times n}$ are the primary-task Jacobian matrix and the secondary task Jacobian matrix, respectively. The general solution of Eq. (5) using the pseudoinverse is as follows:

$$\dot{\mathbf{q}} = \mathbf{J}_p^{\dagger}\dot{\mathbf{x}} + \left(\mathbf{I} - \mathbf{J}_p^{\dagger}\mathbf{J}_p\right)\dot{\mathbf{q}}_0 \tag{7}$$

Substituting Eq. (7) into the secondary task forward velocity kinematics in Eq. (6) yields:

$$\mathbf{J}_s\left(\mathbf{I}-\mathbf{J}_p^{\dagger}\mathbf{J}_p\right)\dot{\mathbf{q}}_0=\dot{\mathbf{x}}_s-\mathbf{J}_s\mathbf{J}_p^{\dagger}\dot{\mathbf{x}}_p \tag{8}$$

Then the unknown $\dot{\mathbf{q}}_0$ that minimizes $\left\|\dot{\mathbf{x}}_s-\mathbf{J}_s\dot{\mathbf{q}}\right\|_2$ is given by:

$$\dot{\mathbf{q}}_0=\widehat{\mathbf{J}}_s^{\dagger}\left(\dot{\mathbf{x}}_s-\mathbf{J}_s\mathbf{J}_p^{\dagger}\dot{\mathbf{x}}_p\right) \tag{9}$$

where $\widehat{\mathbf{J}}_s=\left(\mathbf{J}_s\left(\mathbf{I}-\mathbf{J}_p^{\dagger}\mathbf{J}_p\right)\right)$. The joint space velocities are obtained by substituting Eq. (9) into Eq. (7). Exploiting the fact that the null-space projection operator is Hermitian and idempotent [8], $\dot{\mathbf{q}}$ is found as:

$$\dot{\mathbf{q}}=\mathbf{J}_p^{\dagger}\dot{\mathbf{x}}_p+\left(\mathbf{I}-\mathbf{J}_p^{\dagger}\mathbf{J}_p\right)^{\dagger}\widehat{\mathbf{J}}_s^{\dagger}\left(\dot{\mathbf{x}}_s-\mathbf{J}_s\mathbf{J}_p^{\dagger}\dot{\mathbf{x}}_p\right) \tag{10}$$

However, Eq. (10) is vulnerable to the occurrence of kinematic and algorithmic singularities. A kinematic singularity corresponds to a loss in the manipulator degree of freedom and a drop in the level of redundancy in the system. The primary Jacobian pseudoinverse is given by:

$$\mathbf{J}_p^{\dagger}=\sum_{i=1}^{r}\mathbf{v}_i\mathbf{u}_i^T/\sigma_i \tag{11}$$

where $\mathbf{v}_i$ and $\mathbf{u}_i$ are the right and left singular vectors of $\mathbf{J}_p$, respectively [11]. Hence, one can detect the occurrence of kinematic singularity by monitoring the corresponding singular value σ_r. At the singular configuration, the joint-space velocities along $\mathbf{v}_r$ fall in the null-space of $\mathbf{J}_p$, and as a result the end-effector velocities along $\mathbf{u}_r$ become unrealizable [7].

An algorithmic singularity occurs when the matrix $\widehat{\mathbf{J}}_s=\left(\mathbf{J}_s\left(\mathbf{I}-\mathbf{J}_p^{\dagger}\mathbf{J}_p\right)\right)$ becomes rank deficient. At an algorithmic singularity, the null space of the primary task and the secondary task are linearly dependent, i.e., $N\left(\mathbf{J}_p\right)\cap N\left(\mathbf{J}_s\right)\neq 0$, reflecting the fact that the primary and secondary tasks can not be satisfied simultaneously. In this case high joint velocities and oscillations occur [7]. In order to circumvent the algorithmic singularity problem, the components of the secondary task solution that conflict with the primary task solution must be removed.

2.5 Singularity Robust Task Priority Redundancy Solution

To alleviate the kinematic singularity problem in Eq. (10), the damped-least squares inverse given as $\mathbf{J}_p^{*}=\sum_{i=1}^{r}\left(\sigma_i/(\sigma_i^2+\eta^2)\right)\mathbf{v}_i\mathbf{u}_i^T$ is used in lieu of the pseudoinverse [16]. A non-null damping factor $\eta\in\mathbb{R}$ prevents the denominator from becoming zero. Thus, it provides continuity and good conditioning to the solution, but this improvement is obtained at the expense of an increased residual error.

To alleviate algorithmic singularities, the general solution for the primary task, Eq. (7), can be equalized to the minimum-norm solution of the secondary task, $\mathbf{J}_s^{\dagger}\dot{\mathbf{x}}_s$, to obtain a solution that solves both the primary and secondary task simultaneously [7]:

$$\mathbf{J}_s^{\dagger}\dot{\mathbf{x}}_s=\mathbf{J}_p^{\dagger}\dot{\mathbf{x}}_p+\left(\mathbf{I}-\mathbf{J}_p^{\dagger}\mathbf{J}_p\right)\dot{\mathbf{q}}_0 \tag{12}$$

Eq. (12) can be solved for $\dot{\mathbf{q}}_0$ yielding:

$$\dot{\mathbf{q}}_0=\left(\mathbf{I}-\mathbf{J}_p^{\dagger}\mathbf{J}_p\right)^{\dagger}\left(\mathbf{J}_s^{\dagger}\dot{\mathbf{x}}_s-\mathbf{J}_p^{\dagger}\dot{\mathbf{x}}_p\right) \tag{13}$$

Since $\left(\mathbf{I}-\mathbf{J}_p^{\dagger}\mathbf{J}_p\right)^{\dagger}=\left(\mathbf{I}-\mathbf{J}_p^{\dagger}\mathbf{J}_p\right)$ and $\mathbf{J}_p^{\dagger}=\mathbf{J}_p^{\dagger}\mathbf{J}_p\mathbf{J}_p^{\dagger}$, Eq. (13) can be simplified to:

$$\dot{\mathbf{q}}_0 = \left(\mathbf{I} - \mathbf{J}_p^{\dagger}\mathbf{J}_p\right)\mathbf{J}_s^{\dagger}\dot{\mathbf{x}}_s \tag{14}$$

Substituting Eq. (14) into Eq. (7) and using the idempotence of $\left(\mathbf{I} - \mathbf{J}_p^{\dagger}\mathbf{J}_p\right)$ yields:

$$\dot{\mathbf{q}} = \mathbf{J}_p^{\dagger}\dot{\mathbf{x}}_p + \left(\mathbf{I} - \mathbf{J}_p^{\dagger}\mathbf{J}_p\right)\mathbf{J}_s^{\dagger}\dot{\mathbf{x}}_s \tag{15}$$

In Eq. (15) the minimum-norm solutions to the primary and secondary inverse kinematic problems, Eq. (5) and Eq. (6) respectively, are obtained using the pseudoinverse of the corresponding Jacobian. The joint velocities computed for the secondary task are then projected onto the null space of the primary task to remove components in conflict with the primary task. This provides robustness in the presence of algorithmic singularities. To incorporate the robustness to the kinematic singularities, $\mathbf{J}^{*}$ is used instead of $\mathbf{J}^{\dagger}$ in Eq. (15). However, in URVM applications, $\mathbf{J}_p^{\dagger}$ is used as it is, since the primary Jacobian of the URVM system will always exhibit full rank due to the mobility of the URV [5]. The extension of Eq. (15) to highly redundant systems performing more than two tasks is presented in [13].

The direct implementation of Eq. (15) is prone to a numerical drift occurring when the joint rates are integrated forward in time to obtain URV/manipulator position values. In order to avoid this problem, the closed-loop version of Eq. (15) can be employed [5]:

$$\dot{\mathbf{q}} = \mathbf{J}_p^{\dagger}\left(\dot{\mathbf{x}}_p + \mathbf{K}_P\mathbf{e}_P\right) + \left(\mathbf{I} - \mathbf{J}_p^{\dagger}\mathbf{J}_p\right)\mathbf{J}_s^{\dagger}\left(\dot{\mathbf{x}}_s + \mathbf{K}_s\mathbf{e}_s\right) \tag{16}$$

where $\mathbf{K}_p$ and $\mathbf{K}_s$ are user-defined positive definite matrix gains, and $\mathbf{e}_p$ and $\mathbf{e}_s$ are the numerical construction errors defined as $\mathbf{x}_{p,d} - \mathbf{x}_p$ and $\mathbf{x}_{s,d} - \mathbf{x}_p$ with d denoting the desired values.

3 SINGULARITY ROBUST TASK PRIORITY FOR URVM SYSTEMS

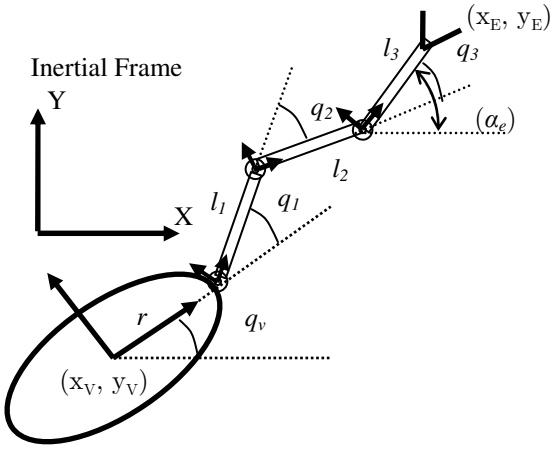

Figure 1: The kinematic chain of the planar underwater vehicle system with a 3 DOF manipulator.

The URV system considered in this work is the Canadian Scientific Submersible Facility's ROPOS equipped with a 3-DOF manipulator as shown in Figure 1. For the sake of simplicity, only a planar end-effector task is considered. The state vector is given as $\mathbf{q} = [x_v \quad y_v \quad q_v \quad q_1 \quad q_2 \quad q_3]^T$, where x_v and y_v are the coordinates of the vehicle's center of mass expressed in the inertial frame, q_v is the yaw angle of the vehicle, and q_i is the joint position with respect to the body-fixed link coordinate system. The terms x_e and y_e are the coordinates of the end-effector, and α_e is the orientation of the end-effector. The distance from the center of mass of the vehicle to the first joint is $r = 1$ m. The distance from one link to another is denoted by l_i, and its values is 1m as well. The primary task is to make the end-effector follow

a predetermined trajectory. Therefore, the corresponding manipulation vector for the primary task is defined as $\mathbf{x}_p = [x_e \quad y_e]^T$. A series of waypoints were set for the end-effector and a continuous set of end-effector values were generated using a quintic polynomial function with zero initial and final velocities. The system starts from the initial configuration of $\mathbf{q} = [0 \quad 0 \quad 0 \quad \pi/3 \quad -\pi/3 \quad \pi/3]^T$ m, rad that corresponds to the end-effector position of $\mathbf{x}_p = [3, \quad 1.7321]^T$ m. The final end-effector location is $\mathbf{x}_p = [5, \quad 5.1962]^T$ m.

The secondary task variables are defined as $\mathbf{x}_s = [x_v \quad y_v \quad q_v]^T$. Note that this definition always leads to a full rank secondary task Jacobian matrix, $\mathbf{J}_s$. Provided the primary task can be tracked using only the manipulator joints, it is desired to keep the URV location constant. To this end, the current URV position value is entered as the desired position values for the next step. This guarantees the zero-URV motion as long as the desired end-effector location is within the current reach of the manipulator.

Since the URV and the manipulator have different dynamic characteristics, it is desired to perform slow URV motions in comparison to the manipulator joint motions. To this end, instead of using the regular pseudoinverse in Eq. (16), a weighted pseudoinverse can be used. The weighted pseudoinverse of the Jacobian that instantaneously minimizes $\|\dot{\mathbf{q}}\|_{\mathbf{W}} = \sqrt{\dot{\mathbf{q}}^T \mathbf{W} \dot{\mathbf{q}}}$ is defined as:

$$\mathbf{J}_w^{\dagger} = \mathbf{W}^{-1}\mathbf{J}^T \left(\mathbf{J}\mathbf{W}^{-1}\mathbf{J}^T\right)^{-1} \tag{17}$$

where $\mathbf{W} = diag\,(w_1, w_2, \ldots, w_n)$ is the positive definite matrix of weight factors for each degree of freedom in a robotic system. For the current implementation, the weight matrix was chosen to be $\mathbf{W} = diag\,(10 \quad 10 \quad 10 \quad 1 \quad 1 \quad 1)$. In the weighting matrix, bigger diagonal values require smaller movements, whereas smaller values require larger movements for the associated degree of freedom.

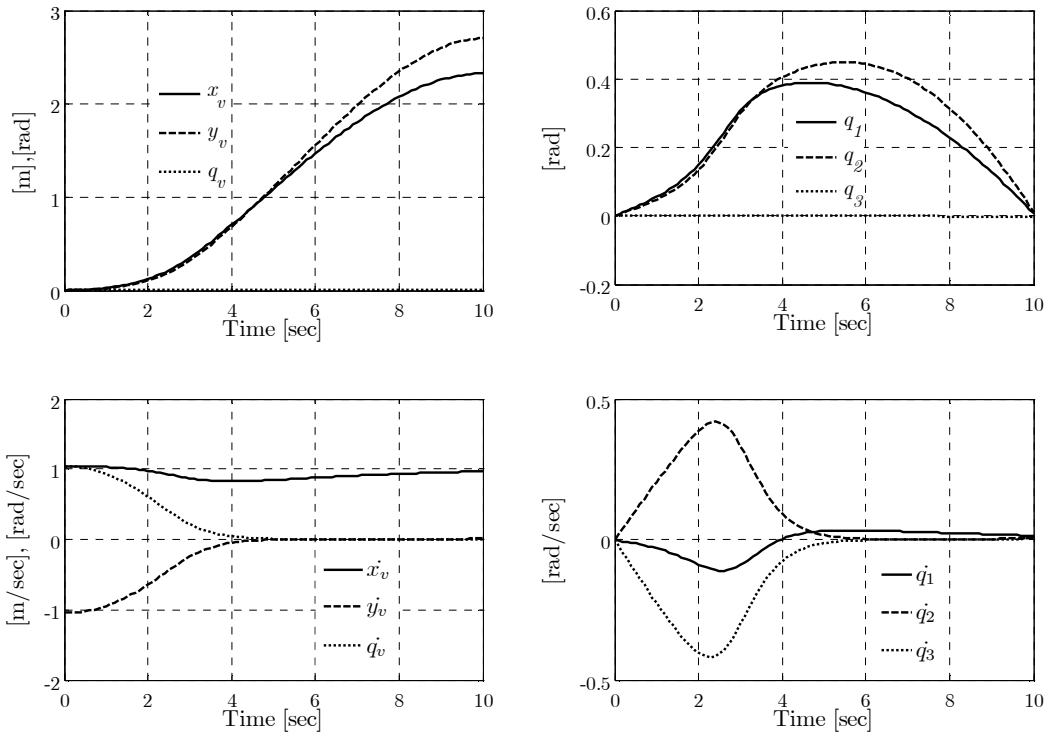

Figure 2: Time history of state variables for the URV (left figures) and the manipulator (right figures).

In the simulation, Eq. (16) is used with $\mathbf{K}_p = [10 \quad 10]^T$ and $\mathbf{K}_s = [10 \quad 10 \quad 100]^T$. Figure 2 reports the simulation results. As the figures reveal, the primary task is successfully achieved. The scheme produced

joint positions and velocities that are realizable, as they show a smooth pattern, with no jerk. However, despite the secondary task constraint, the URV moved during the manoeuvre; indicating that the trajectory goes out of the workspace of the sole manipulator. As can be seen from Figure 3, the singularity robust task-priority approach drives the sole manipulator into its singular configuration, i.e., stretched-out configuration for the current simulation case.

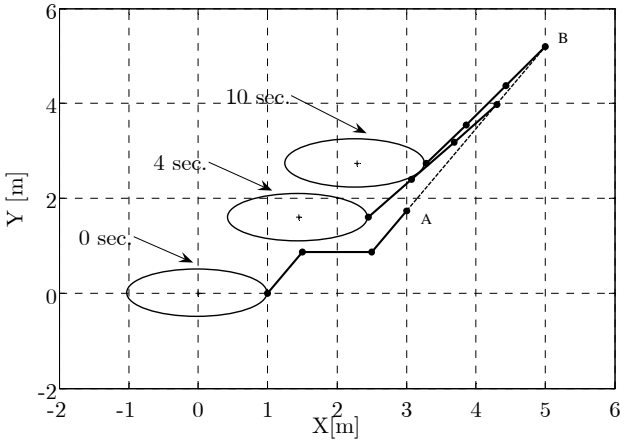

Figure 3: System configuration during the URVM manoeuvre.

The primary Jacobian of the URVM system will always exhibit full rank due to the mobility of the URV [5]. This implies that the kinematic structure of the URVM system precludes singular configurations. However, with this arrangement, the sole manipulator singularities are still problematic due to the reasons given in Section 1. Therefore, prevention of manipulator singularities must be included in the framework of the redundancy resolution method. In the following section, this constraint is added to the current task priority approach.

4 AVOIDING MANIPULATOR SINGULARITIES

4.1 Overview

It has been shown that the singularity task priority approach as given in Section 2.5 is not suitable for the URVM system since it might drive the manipulator component into its singular configurations. In the following sections, the method proposed to circumvent this problem will be presented.

4.2 Measure of Manipulability

There is a strong connection between the kinematic singularities of the sole manipulator and the algorithmic singularities of the URVM system for the current application. The algorithmic singularities occur when $\mathbf{J}_p$ and $\mathbf{J}_s$ have common linearly dependent rows or columns meaning the primary and secondary tasks are in conflict [15]. Given that the secondary task is to keep the URV at the current location, any conflict indicates that the end-effector can not be placed at a desired location without using the URV's mobility. This happens when a loss in the degree of freedom of the manipulator, a kinematic singularity, is experienced during the URV station keeping. In an effort to monitor the kinematic singularity of the sole manipulator, it is proposed that the collective Jacobian matrix $\mathbf{J}_a = [\mathbf{J}_p^T \quad \mathbf{J}_s^T]^T$ be used. The rank deficiency of $\mathbf{J}_a$ indicates a conflict in the primary and the secondary task since $\mathbf{J}_p$ and $\mathbf{J}_s$ always have full rank. Consequently, $\mathbf{J}_a$ can be used as the indicator of the sole manipulator singularity.

In an attempt to track the singularity, it is useful to use a parameter that quantifies the closeness to the singular configurations. Yoshikawa [14] proposed that the measure of manipulability

$$\rho = \sqrt{\det\left[\mathbf{J}_a \mathbf{J}_a^T\right]} \tag{18}$$

be used for this purpose. Using the singular value decomposition of the Jacobian matrix, $\mathbf{J}_a = \mathbf{U}\Sigma\mathbf{V}^T$, it can be shown that Eq. (18) is merely the product of the singular values, $\rho = \prod_{i=1}^{m} |\sigma_i|$ [18]. The measure of manipulability becomes zero only when the Jacobian matrix is not full rank.

In order to monitor how the measure of manipulability changes with respect to the joint vector, the following equation can be used [17]:

$$\frac{\partial \rho}{\partial q_i} = \rho \cdot trace\left(\frac{\partial \mathbf{J}_a}{\partial q_i}\mathbf{J}_a^{\dagger}\right), \quad i = 1\ldots n \tag{19}$$

It is also desirable to know how ρ evolves in time when Eq. (15) is used to solve the redundancy:

$$\frac{d\rho}{dt} = \frac{\partial \rho}{\partial \mathbf{q}}\dot{\mathbf{q}}^T = \frac{\partial \rho}{\partial \mathbf{q}}\left(\mathbf{J}_p^{\dagger}\dot{\mathbf{x}}_p + \left(\mathbf{I} - \mathbf{J}_p^{\dagger}\mathbf{J}_p\right)\mathbf{J}_s^{\dagger}\dot{\mathbf{x}}_s\right)^T \tag{20}$$

4.3 Dexterous Dynamic Task Priority Approach

The following redundancy resolution is proposed:

$$\dot{\mathbf{q}} = \mathbf{J}_{w,p}^{\dagger}\left(\dot{\mathbf{x}}_p + \mathbf{K}_P\mathbf{e}_P\right) + \left(\mathbf{I} - \mathbf{J}_{w,p}^{\dagger}\mathbf{J}_p\right)\left((1-k)\mathbf{J}_s^{\dagger}\left(\dot{\mathbf{x}}_s + \mathbf{K}_s\mathbf{e}_s\right) + k\left(\frac{1 - sign\left(\frac{d\rho}{dt}\right)}{2}\right)\left(\lambda\frac{\partial \rho(\mathbf{J}_a)}{\partial \mathbf{q}}\right)\right) \tag{21}$$

where $\mathbf{J}_w^{\dagger}$ is the weighted pseudoinverse, $\mathbf{J}_{w,p}$ is the weighted Jacobian given as $\mathbf{J}_{w,p} = \mathbf{J}_p\mathbf{W}^{-1/2}$, λ is a arbitrarily defined positive constant determining the convergence rate to the local minimum of the measure of manipulability function, and k is the shaping function [18];

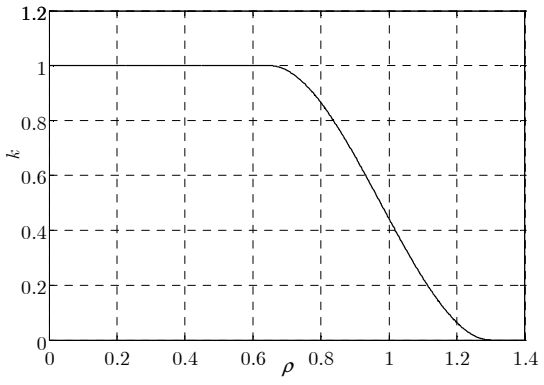

$$k = \begin{cases} 0 & \bar{\rho} \le \rho \\ 4\left(\dfrac{4\rho^3 - 9\rho^2\bar{\rho} + 6\bar{\rho}^2\rho - \bar{\rho}^3}{\bar{\rho}^3}\right), & \dfrac{\bar{\rho}}{2} \le \rho < \bar{\rho} \\ 1 & \rho < \dfrac{\bar{\rho}}{2} \end{cases}$$

Figure 4: Shaping function definition (right) and corresponding plot for $\bar{\rho} = 1.3$ (left).

A threshold value $\bar{\rho}$ determined based on the desired proximity from singular configurations is set on the measure of manipulability. Equation (21) can be thought of as the combination of the gradient projected method and the singularity robust task-priority approach. When activated, it works to move the manipulator away from the singular configurations. The task-priority component works as in Section 2.5, keeping the URV at the current location in an effort to provide a stable platform for the end-effector task.

In order to blend the task priority and projected gradient contributions, a shaping function is used to distribute the secondary task demand over the station-keeping and the singularity avoidance tasks. If the

measure of manipulability is bigger than the designated threshold, *k* becomes zero, and Eq. (21) becomes equivalent to the task-priority approach of Section 3. In cases where $\bar{\rho}/2 \le \rho < \bar{\rho}$, the shaping function distributes the secondary task demand. When the measure of manipulability drops below half of the threshold, then the emphasis is fully placed on the singularity avoidance. In this case, the URV-related secondary task is fully disregarded, and the available redundancy, including the URV's mobility, is committed fully to the manipulator's singularity avoidance. However, the intervention of the projected gradient solution is not necessary when ρ is naturally increasing. As such, a discontinuous switching term, using the *sign* function defined as for $\dot{\rho} \le 0$, $sign(\dot{\rho}) = -1$ and for $\dot{\rho} > 0$, $sign(\dot{\rho}) = 1$, is added such that the singularity avoidance only intervenes in times of worsening manipulability.

4.4 APPLICATION TO URVM SYSTEM

The proposed method was implemented to the URVM system for the same simulation parameters described in Section 3. Equations (21) is implemented with λ=10 and $\bar{\rho}$=1.3. The simulation results are reported in Figure 5. As can be seen the figure, the primary task was successfully executed. As opposed to the robust task priority approach, the proposed scheme does not force the manipulator component to hit its singular straight arm configuration. As can be seen in Figure 6, when the manipulator approaches a singular configuration, the system reconfigures itself in a dexterous configuration using the URV's mobility. The reconfiguration takes place while the URV provides a stable platform for the manipulator as much as possible; the URV moves along translational directions since it is unavoidable, but the rotational motion is prevented in agreement with the secondary task. Therefore, Eq. (21) provides a means to increase the dexterity of the manipulator in an optimal, coordinated manner.

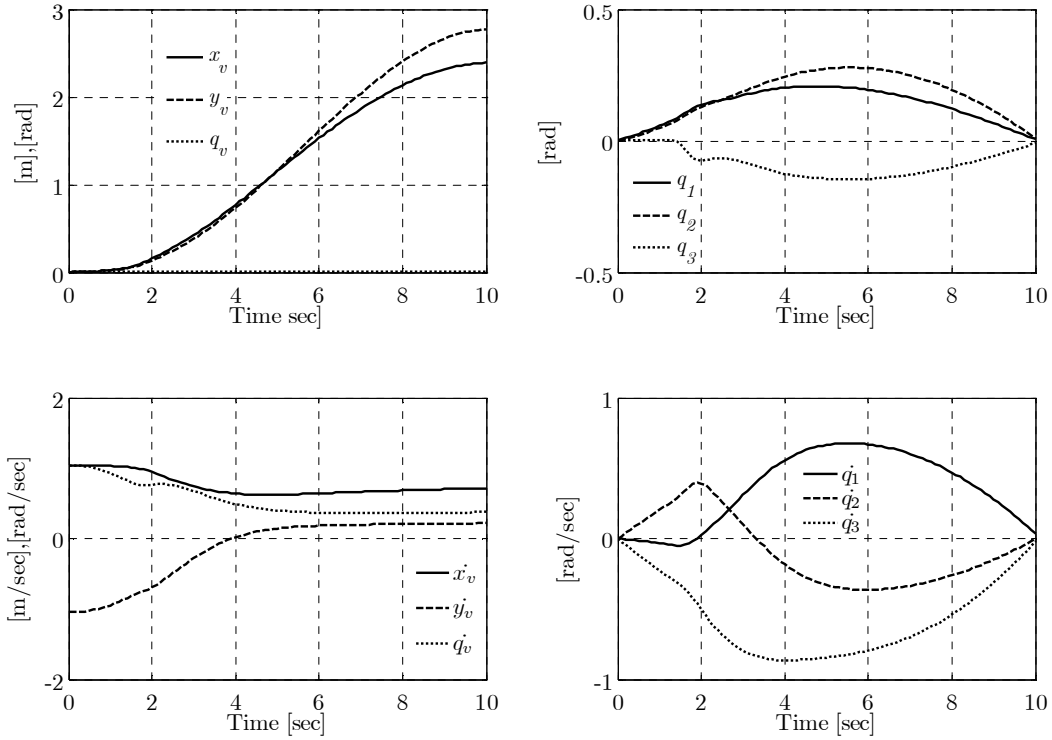

Figure 5: Time history of state variables for the URV (left figures) and the manipulator (right figures).

The left figure in Figure 7 reveals that the robust task-priority redundancy resolution, Eq. (16), leads to poor dexterity performance; it falls into near singularity at approximately 5 seconds. The measure of manipulability never reaches the zero value due to the mobility of the URV, but the system dexterity is still very poor. The right figure in Figure 7 is obtained from the implementation of Eq. (21). As the figure reveals, the dexterity of the system is significantly improved. The lower bound $\bar{\rho}$=1.3 determines the

extent to which the system reconfigures itself in an effort to avoid manipulator singularities. This value can be adjusted on-line depending on the specific requirements of a given task.

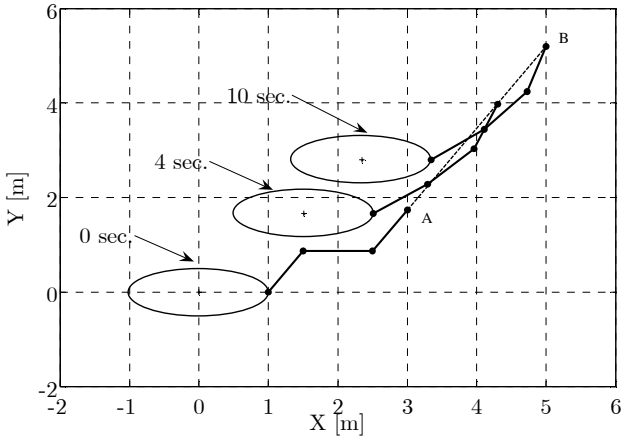

Figure 6: Along the trajectory, the manipulator avoids its singular configurations.

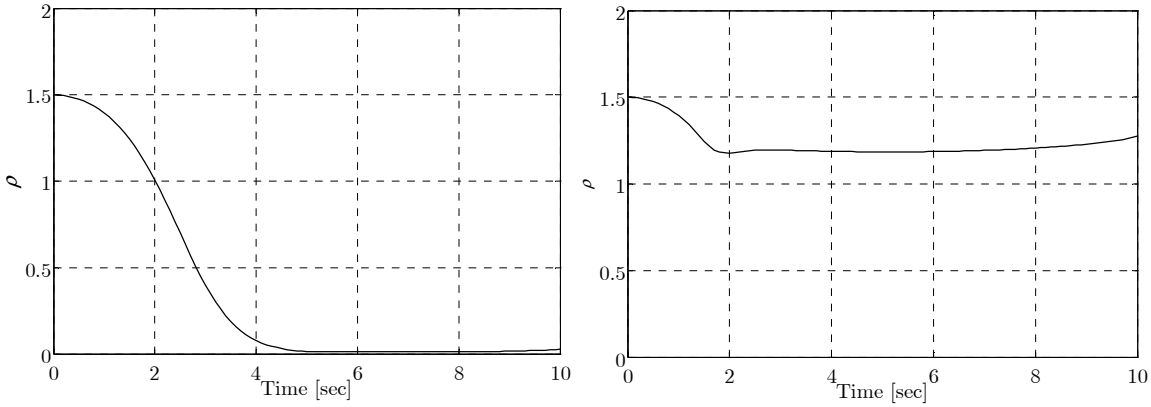

Figure 7: Measure of manipulability for the task priority approach (left) and the task priority approach augmented with manipulability monitoring.

5 CONCLUSION

This work has addressed the problem of kinematic redundancy in URVM systems. To solve the problem, the robust task-priority approach was implemented first. It has been shown that the robust task-priority approach is not suitable for URVM application since it causes the manipulator component to approach singular configurations. The singular configurations of the sole manipulator cause the same significant complications for the manipulator controller as in land-based non-redundant cases. In order to solve this problem, a new heuristic method has been proposed and implemented that uses a manipulability measure to slowly apply URV motions in an optimal, coordinated manner through a simple shaping function. This removes the complexity associated with the existing solutions to the singularity problem. The method presented produces URV-manipulator state values that significantly improve the dexterity of the system, and thus ensures dexterous manipulation. This scheme makes the prevailing task-priority approach more suitable, and hence improves the coordinated control of the URVM systems.

ACKNOWLEDGEMENT

The authors wish to thank the Natural Sciences and Engineering Research Council (NSERC) of Canada for providing financial support for this research.

REFERENCES

[1] M. W. Dunnigan, and G. T. Russell, "Evaluation and reduction of the dynamic coupling between a manipulator and an underwater vehicle," *IEEE Journal of Oceanic Engineering*, vol. 23, no. 3, pp. 260-273, July 1998.

[2] G. Grenon, P. An, S. Smith, A. Healey, "Enhancement of the inertial navigation system for the Morpheus autonomous underwater vehicles," *IEEE J. Oceanic Eng.*, vol. 26 no. 4, pp. 548-560, Oct. 2001.

[3] J. Kim and W. K. Chung, "Dynamic analysis and two-time scale control for underwater vehicle-manipulator systems," *Proc. 2003 IEEE/RSJ Int. Conf. Intelligent Robots and Systems, (IROS 2003)*, vol:1, pp. 577–582, 2003.

[4] S. Soylu, B. J. Buckham and R. P. Podhorodeski, "Using articulated-body algorithm within sliding mode control to compensate dynamic coupling in underwater manipulator systems," *CSME Trans. 2005 Special Edition*, June 2006.

[5] G. Antonelli, and S. Chiaverini, "Fuzzy redundancy resolution and motion coordination for underwater vehicle-manipulator systems, "*IEEE Trans. on Fuzzy Syst*., vol. 11, no. 1, pp. 109-120, 2003.

[6] G. Antonelli and S. Chiaverini, "Task priority redundancy resolution for underwater-manipulator systems," *Proc. 1998 IEEE Int. Conf. Robotics Automation*, pp. 768-733, May 1998.

[7] S. Chiaverini, "Singularity-robust task-priority redundancy resolution for real-time kinematic control of robot manipulators, "*IEEE Trans. Robotics Automation*. vol. 13, pp. 398-410, June 1997.

[8] A. A. Maciejewski, and C. A. Klein, "Obstacle avoidance for kinematically redundant manipulators in dynamically varying environments," *The Int. J. Robot. Res.,* vol. 4, no.3, pp. 109-117, 1985.

[9] Y. Nakamura, H. Hanafusa, and T. Yoshikawa, "Task-priority based redundancy control of robot manipulators," *The Int. J. Robot. Res.*, vol. 6, no. 2, pp. 3-15, 1987.

[10] N. Sarkar and T. K. Podder, "Motion coordination of underwater vehicle-manipulator systems subject to drag optimization," *Proc. 1999 IEEE Int. Conf. Robotics Automation*, pp. 387-392, 1999.

[11] D. S. Watkins, Fundamentals of Matrix Computations, 2nd Edition, John Wiley&Sons, 2002.

[12] A. Liegeois, "Automatic supervisory control of the configuration and behaviour of multibody mechanisms," *IEEE Trans. Syst., Man, Cybern*., vol. SMC-7, pp. 868-871, 1977.

[13] B. Siciliano and J. J. E. Slotine, "A general framework for managing multiple tasks in highly redundant robotic systems," *Proc. Int. Conf. Advanced Robotics*, Pisa, Italy, pp. 1211-1216, June 1991.

[14] T. Yoshikawa, "Manipulability of robotic mechanisms," *Int. J. of Robotic Research*, vol. 4, no.2, pp.3-9, 1985.

[15] H. Seraji and R. Colbaugh, "Singularity-robustness and task-prioritization in configuration control of redundant robots," *Proc. 29th IEEE Conf. on Decision and Control*, pp. 3089-3095, 1990.

[16] Y. Nakamura and H. Hanafusa, "Inverse kinematic solutions with singularity robustness for robot manipulator control, "*Trans. ASME J. Dynamic Syst., Measure., Contr*., vol. 108, pp. 163-171, 1986.

[17] J. Park, "*Analysis and control of kinematically redundant manipulators: An approach based on kinematically decoupled joint space decomposition,*" PhD thesis, Pohang University of Science and Technology (POSTECH), 1999.

[18] G. Marani, J. Kim, J. Yuh, W. K. Chung, "Algorithmic singularities avoidance in task-priority based controller for redundant manipulators," *Proc. 2003 IEEE/RSJ Int. Conf. on Intelligent Robots and Systems,* Las Vegas, pp.3570-3574, Oct. 2003.